DESIGN OF BI-METALLIC DEVICES BASED ON THE TOPOLOGICAL DERIVATIVE CONCEPT

S.M. GIUSTI AND A.A. NOVOTNY

Abstract. In this work the topological derivative concept is applied in the context of topology design of thermo-mechanical devices, where the linear elasticity system (modeled by the Navier equation) is coupled with the steady-state heat conduction problem (modeled by the Laplace equation). The mechanical coupling term comes out from the thermal stress induced by the temperature field. We consider the topology design of bi-metallic devices. The idea is to maximize the displacement in a given direction defined on the boundary of the thermo-elastic body with respect to a bi-metallic material distribution. The topological derivative is obtained by considering the nucleation of a small circular inclusion with different thermal expansion coefficients. A level-set domain representation method is used, together with the derived topological sensitivity formula, to devise a topology design algorithm. Finally, some numerical experiments regarding the conceptual design of thermo-mechanical devices are presented.

1. Introduction

In this paper we are interested in the topology design of thermo-mechanical devices, which consist of multi-flexible structures that generate an output displacement in a specified direction produced by thermal expansions/contractions. In particular, the linear elasticity system (modeled by the Navier equation) is coupled with the steady-state heat conduction problem (modeled by the Laplace equation). The mechanical coupling term comes out from the thermal stress induced by the temperature field. Since the multi-flexible structure transforms the thermal expansion/contraction output displacement by amplifying and changing its direction, then the basic idea consists in maximizing the displacement in a given direction defined on the boundary of the thermo-elastic body with respect to a bi-metallic material distribution.

However, the development of such thermo-mechanical devices requires the design of multi-flexible structures which are able to produce complex movements originated from simple expansion/contraction thermal effects. In particular, the performance of these devices can be strongly enhanced by optimizing the multi-flexible structures with respect to their shape and their topology. A quite general approach to deal with shape and topology optimization design is based on the topological derivative. In fact, this relatively new concept represents the first term of the asymptotic expansion of a given shape functional with respect to the small parameter which measures the size of singular domain perturbations, such as holes, inclusions, source-terms and cracks. The topological asymptotic analysis was introduced in the fundamental paper [10] and has been successfully applied in the treatment of problems such as topology optimization [4], inverse analysis [7], image processing [6], multi-scale constitutive modeling [3], fracture mechanics sensitivity analysis [12] and damage evolution modeling [1]. For an account of new developments in this branch of shape optimization we refer to the book by Novotny & Sokołowski [9].

The topological derivative concept is applied here in the context of topology optimization design of thermo-mechanical devices. The performance of the multi-flexible thermo-elastic structure is maximized by introducing a set of small inclusions with different thermal expansion coefficients only. For the sake of simplicity, we consider that the elastic properties remains fixed, allowing to avoid complicated derivations such as the ones presented in [5], where the topological asymptotic expansion of the strain energy stored in a thermo-mechanical device, associated with singular perturbations in the elastic, thermal conductivity and thermal expansion coefficients, has been derived. In particular, here the topological derivative, obtained in its closed form, is

Key words and phrases. topological derivative, topology optimization design, thermo-mechanical devices/actuators.

used as a steepest descent direction in a topology design algorithm of thermo-mechanical devices. Therefore, the simplified obtained result shall be useful in the conceptual design of such multi-flexible structures.

The paper is organized as follows. The optimal problem consisting in maximizing the performance of thermo-mechanical devices is stated in Section 2. The associated topological asymptotic analysis with respect to the nucleation of a small inclusion with different thermal expansion coefficient is developed in Section 3. Finally, several numerical results associated with topology design of bi-metallic devices are presented in Section 4. The paper ends in Section 5 with some concluding remarks.

2. Problem Formulation

In this section the optimization problem in which we are dealing with is introduced. It consists in maximizing the displacement in a given direction defined on the boundary of the thermo-elastic body with respect to a bi-metallic material distribution. Thus, let us consider an open and bounded domain $\Omega \in \mathbb{R}^2$, with boundary $\partial\Omega$, representing an elastic solid body subject to thermo-mechanical deformation effects. The following shape functional is introduced:

$$\mathcal{G}(u) := -\int_{\Gamma^\star} e \cdot u \,, \tag{2.1}$$

where e is a given direction prescribed on the boundary $\Gamma^\star \subset \partial\Omega$. The thermal-mechanical displacement u is solution to the following *thermo-mechanical* variational problem

$$u \in \mathcal{U}^M \;:\; \int_\Omega \sigma(u) \cdot \nabla\eta^s = \int_\Omega Q(\theta) \cdot \nabla\eta^s \quad \forall \eta \in \mathcal{V}^M. \tag{2.2}$$

The displacement field on the boundary $\Gamma_D \subset \partial\Omega$ satisfies $u_{|\Gamma_D} = \bar{u}$, being $\bar{u}$ a prescribed displacement. Therefore, the set $\mathcal{U}^M$ and the space $\mathcal{V}^M$ are defined as

$$\mathcal{U}^M := \left\{\varphi \in H^1(\Omega;\mathbb{R}^2) : \varphi_{|\Gamma_D} = \bar{u}\right\} \quad \text{and} \quad \mathcal{V}^M := \left\{\varphi \in H^1(\Omega;\mathbb{R}^2) : \varphi_{|\Gamma_D} = 0\right\}. \tag{2.3}$$

We assume that $\Gamma^\star \cap \Gamma_D = \varnothing$. The Cauchy stress tensor $\sigma(u)$ is defined as:

$$\sigma(u) := \mathbb{C}\nabla u^s \,, \tag{2.4}$$

where ∇u^s is used to denote the symmetric part of the gradient of the displacement field u, i.e.

$$\nabla u^s := \frac{1}{2}(\nabla u + (\nabla u)^\top) \,. \tag{2.5}$$

The induced thermal stress tensor $Q(\theta)$ is defined as:

$$Q(\theta) := \mathbb{C}B\theta \,. \tag{2.6}$$

In addition, $\mathbb{C}$ denotes the four-order elasticity tensor and B denotes the second-order thermo-elastic coupled tensor. In the case of isotropic elastic body, theses tensors are given by:

$$\mathbb{C} = 2\mu\mathbb{I} + \lambda(I \otimes I) \quad \text{and} \quad B = \alpha I \quad \Rightarrow \quad \mathbb{C}B = 2\alpha(\lambda+\mu)I, \tag{2.7}$$

with μ and λ denoting the Lame's coefficients, and α the thermal expansion coefficient. In terms of the Young's modulus E and Poisson's ratio ν the above constitutive response can be written as:

$$\mathbb{C} = \frac{E}{1-\nu^2}[(1-\nu)\mathbb{I} + \nu(I \otimes I)] \quad \text{and} \quad \mathbb{C}B = \frac{\alpha E}{1-\nu} I \,. \tag{2.8}$$

Finally, the temperature field θ in (2.2) is solution to the following variational problem

$$\theta \in H^1_0(\Omega) \;:\; \int_\Omega q(\theta) \cdot \nabla\eta = \int_\Omega b\eta \quad \forall \eta \in H^1_0(\Omega), \tag{2.9}$$

where b is a prescribed distributed heat source in Ω. The heat flux operator $q(\theta)$ is defined as

$$q(\theta) = -K\nabla\theta, \tag{2.10}$$

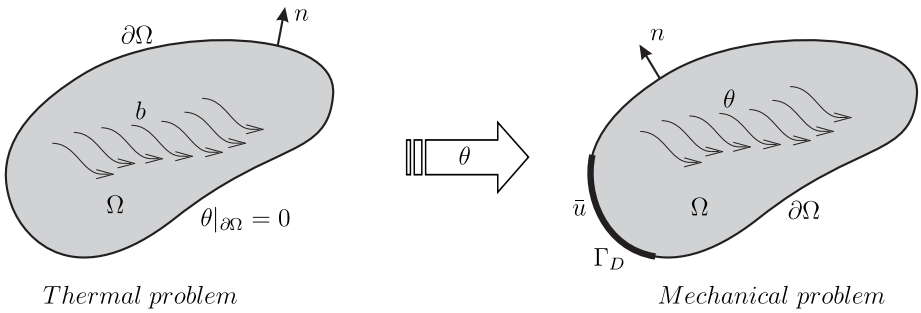

FIGURE 1. Thermo-mechanical semi-coupled problem.

where K is a second order tensor representing the thermal conductivity of the medium. In the isotropic case, tensor K can be written as

$$K = kI \,, \tag{2.11}$$

being k the thermal conductivity coefficient. See details of the coupled system in Fig. 1. Therefore, our optimization problem can be written as:

$$\text{Minimize } \mathcal{G}(u) \,, \quad \text{subject to} \quad (2.2) \,. \tag{2.12}$$

3. Topological asymptotic analysis

The topological derivative with respect to the nucleation of a small circular inclusion with different thermal expansion coefficient is now derived. This derivative represents the first order term of the topological asymptotic expansion of a shape functional with respect to an infinitesimal singular domain perturbation. See, for instance, [9].

In order to introduce these ideas, we consider that the domain Ω is submitted to a non-smooth perturbation confined in a small region $\mathcal{B}_\varepsilon(\widehat{x})$ of size ε with center at an arbitrary point $\widehat{x} \in \Omega$. Thus, let us introduce a characteristic function $\chi = \mathbb{1}_\Omega$ associated to the unperturbed domain, so that it is possible to define a characteristic function associated to the topological perturbed domain in the form $\chi_\varepsilon(\widehat{x}) = \mathbb{1}_\Omega - (1-\gamma)\mathbb{1}_{\overline{\mathcal{B}_\varepsilon(\widehat{x})}}$, where $\gamma \in \mathbb{R}^+$ is the contrast parameter in the material property of the medium, see Fig. 2. Then we assume that a given shape functional $\psi(\chi_\varepsilon(\widehat{x}))$, associated to the topological perturbed domain, admits the following topological asymptotic expansion

$$\psi(\chi_\varepsilon(\widehat{x})) = \psi(\chi) + f(\varepsilon) D_T\psi(\widehat{x}) + o(f(\varepsilon)) \,, \tag{3.1}$$

where $\psi(\chi)$ is the shape functional associated to the unperturbed domain, $f(\varepsilon)$ is a function such that $f(\varepsilon) \to 0^+$, with $\varepsilon \to 0$. Function $\widehat{x} \mapsto D_T\psi(\widehat{x})$ is the so-called topological derivative of ψ at the point $\widehat{x}$. Thus, the topological derivative can be seen as a first order correction factor over $\psi(\chi)$ to approximate $\psi(\chi_\varepsilon(\widehat{x}))$.

Several methods were proposed to calculate the topological derivative. In this paper, we apply the so-called topological-shape sensitivity method developed in [8], which is based on the following result (see also [9]):

$$D_T\psi(\hat{x}) = \lim_{\varepsilon\to 0} \frac{1}{f'(\varepsilon)} \frac{d}{d\varepsilon}\psi(\chi_\varepsilon(\hat{x})) \,. \tag{3.2}$$

The derivative of $\psi(\chi_\varepsilon(\widehat{x}))$ with respect to ε can be seen as the sensitivity of $\psi(\chi_\varepsilon(\widehat{x}))$, in the classical sense [11], to the domain variation produced by a uniform expansion of the perturbation $\mathcal{B}_\varepsilon$. In fact, we have

$$\frac{d}{d\varepsilon}\psi(\chi_\varepsilon(\widehat{x})) = \lim_{t\to 0} \frac{\psi(\chi_{\varepsilon+t}(\widehat{x})) - \psi(\chi_\varepsilon(\widehat{x}))}{t} \,, \tag{3.3}$$

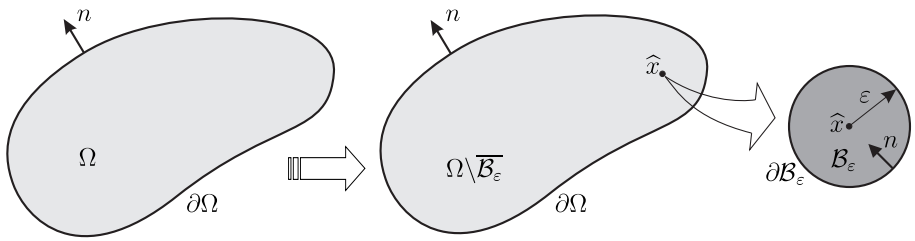

FIGURE 2. Topological derivative concept.

where $\psi(\chi_{\varepsilon+t}(\widehat{x}))$ is the shape functional associated to the perturbed domain, whose perturbation is given by $\mathcal{B}_{\varepsilon+t}$. Therefore, we can use the concept of shape sensitivity analysis as an intermediate step in the topological derivative calculation.

In particular, we consider a contrast only in the thermal expansion coefficient, which drastically simplifies the analysis [5]. Then, the constitutive properties $\mathbb{C}$ and K remains fixed, while the perturbed thermal expansion coefficient is given by:

$$\gamma_\varepsilon B := \left\{ \begin{array}{rcl} B & \text{in} & \Omega \setminus \overline{\mathcal{B}_\varepsilon} \\ \gamma B & \text{in} & \mathcal{B}_\varepsilon \end{array} \right. . \tag{3.4}$$

Then, by considering (3.4), the topologically perturbed problem reads

$$u_\varepsilon \in \mathcal{U}^M \; : \; \int_\Omega \sigma(u_\varepsilon) \cdot \nabla \eta^s = \int_\Omega Q_\varepsilon(\theta) \cdot \nabla \eta^s \quad \forall \eta \in \mathcal{V}^M \; , \tag{3.5}$$

where the perturbed tensor $Q_\varepsilon(\theta)$ takes the form

$$Q_\varepsilon(\theta) := \gamma_\varepsilon \mathbb{C} B \theta = \gamma_\varepsilon Q(\theta) \; . \tag{3.6}$$

Therefore, the shape functional $\mathcal{G}$, defined by (2.1), associated now with the above perturbed problem reads

$$\mathcal{G}(u_\varepsilon) := - \int_{\Gamma^\star} e \cdot u_\varepsilon \, . \tag{3.7}$$

Before proceed with the analysis, let us state the following important result:

Lemma 1. *Let u and u_ε be solutions to the original and perturbed problems respectively given by* (2.2) *and* (3.5)*. Then, the following estimate holds true*

$$\|u_\varepsilon - u\|_{H^1(\Omega;\mathbb{R}^2)} \leq C\varepsilon \; , \tag{3.8}$$

where C is a constant independent of the control parameter ε.

Proof. Let us subtract (2.2) from (3.5). After taking into account the definition of the contrast γ_ε in eq. (3.4), we obtain

$$\int_\Omega \sigma(u_\varepsilon - u) \cdot \nabla \eta^s = (\gamma - 1) \int_{B_\varepsilon} Q(\theta) \cdot \nabla \eta^s \; . \tag{3.9}$$

By taking $\eta = u_\varepsilon - u$ as test function in the above equation, we get

$$\int_\Omega \sigma(u_\varepsilon - u) \cdot \nabla (u_\varepsilon - u)^s = (\gamma - 1) \int_{B_\varepsilon} Q(\theta) \cdot \nabla (u_\varepsilon - u)^s \; . \tag{3.10}$$

From the Cauchy-Schwarz inequality there is

$$\begin{aligned} \int_\Omega \sigma(u_\varepsilon - u) \cdot \nabla (u_\varepsilon - u)^s &\leq C_1 \|Q(\theta)\|_{L^2(B_\varepsilon;\mathbb{R}^2)} \|\nabla (u_\varepsilon - u)^s\|_{L^2(B_\varepsilon;\mathbb{R}^2)} \\ &\leq C_2 \varepsilon \|u_\varepsilon - u\|_{H^1(\Omega;\mathbb{R}^2)} \; , \end{aligned} \tag{3.11}$$

where we have used the interior elliptic regularity of function θ. Finally, from the coercivity of the bilinear form on the left hand side of the above inequality, namely,

$$c \|u_\varepsilon - u\|^2_{H^1(\Omega;\mathbb{R}^2)} \leq \int_\Omega \sigma(u_\varepsilon - u) \cdot \nabla (u_\varepsilon - u)^s \; , \tag{3.12}$$

we obtain

$$\|u_\varepsilon - u\|^2_{H^1(\Omega;\mathbb{R}^2)} \leq C\varepsilon \|u_\varepsilon - u\|_{H^1(\Omega;\mathbb{R}^2)} \,, \tag{3.13}$$

which leads to the result with $C = C_2/c$. □

By taking into account the above result and (3.2), we can state the following theorem:

Theorem 2. *The topological derivative of the shape functional* (2.1) *is given by*

$$D_T\psi(\widehat{x}) = (1-\gamma) B\theta(\widehat{x}) \cdot \sigma(v)(\widehat{x}) \,, \tag{3.14}$$

where the function v is the solution of the following variational problem

$$v \in \mathcal{V}^M \;:\; \int_\Omega \sigma(v) \cdot \nabla \eta^s = \int_{\Gamma^\star} e \cdot \eta \quad \forall \eta \in \mathcal{V}^M. \tag{3.15}$$

Proof. By considering the nucleation of an inclusion $\mathcal{B}_\varepsilon$ in the domain Ω at point $\widehat{x}$, the state equation (2.2) can be written as

$$u_\varepsilon \in \mathcal{U}^M \;:\; \int_\Omega \sigma(u_\varepsilon) \cdot \nabla \eta^s = \int_\Omega Q(\theta) \cdot \nabla \eta^s + (\gamma - 1) \int_{\mathcal{B}_\varepsilon} Q(\theta) \cdot \nabla \eta^s \qquad \forall \eta \in \mathcal{V}^M \,. \tag{3.16}$$

The shape derivative of the cost functional defined by (3.7) can be written as:

$$\dot{\mathcal{G}}(u_\varepsilon) = -\int_{\Gamma^\star} e \cdot \dot{u}_\varepsilon \,, \tag{3.17}$$

where the superimposed dot denotes the (total) material derivative with respect to ε. On the other hand, the derivative of the state equation (3.16) with respect to the parameter ε is given by

$$\dot{u}_\varepsilon \in \mathcal{V}^M \;:\; \int_\Omega \sigma(\dot{u}_\varepsilon) \cdot \nabla \eta^s = (\gamma - 1) \int_{\partial\mathcal{B}_\varepsilon} Q(\theta) \cdot \nabla \eta^s \quad \forall \eta \in \mathcal{V}^M \,. \tag{3.18}$$

By choosing $\eta = v$ as test function in (3.18) we have the equality

$$\int_\Omega \sigma(\dot{u}_\varepsilon) \cdot \nabla v^s = (\gamma - 1) \int_{\partial\mathcal{B}_\varepsilon} Q(\theta) \cdot \nabla v^s \,, \tag{3.19}$$

where v is solution to the auxiliary problem (3.15). On the other hand, by taking $\eta = \dot{u}_\varepsilon$ in (3.15), we obtain the following equality

$$\int_\Omega \sigma(v) \cdot \nabla \dot{u}^s_\varepsilon = \int_{\Gamma^\star} e \cdot \dot{u}_\varepsilon. \tag{3.20}$$

Then, by comparing the last two results we get the following identity

$$\int_{\Gamma^\star} e \cdot \dot{u}_\varepsilon = (\gamma - 1) \int_{\partial\mathcal{B}_\varepsilon} Q(\theta) \cdot \nabla v^s \,, \tag{3.21}$$

where we have considered the symmetry of the bilinear forms. Finally, by introducing the above expression in (3.17) and using the interior elliptic regularity of functions θ and v, we can write

$$\dot{\mathcal{G}}(u_\varepsilon) = (1-\gamma) \int_{\partial\mathcal{B}_\varepsilon} Q(\theta) \cdot \nabla v^s = 2\pi\varepsilon(1-\gamma) Q(\theta)(\widehat{x}) \cdot \nabla v^s(\widehat{x}) + o(\varepsilon^2) \,, \tag{3.22}$$

which leads to the result by setting $f(\varepsilon) = \pi\varepsilon^2$ in (3.2). □

4. Numerical results

The obtained result (3.14) can be combined with a level-set domain representation method for solving the topology optimization problem we are dealing with. The resulting algorithm is now explained in details for the reader convenience. It has been proposed in [2] and consists basically in looking for a local optimality condition for the minimization problem (2.12) written in terms of the topological derivative and a level-set function. Therefore, the domain Ω is divided into two subdomains Ω_1 and Ω_2, representing the thermo-elastic parts with higher and lower thermal

expansion coefficients, respectively. Let us then introduce a level-set function $\Psi \in L^2(\Omega)$ of the form:

$$\Omega_1 = \{\Psi(x) < 0 \text{ a.e. in } \Omega\} \quad \text{and} \quad \Omega_2 = \{\Psi(x) > 0 \text{ a.e. in } \Omega\} \,, \tag{4.1}$$

where Ψ vanishes on the interface between both subdomains. A local sufficient optimality condition for Problem (2.12), under the considered class of domain perturbation given by circular inclusions, can be stated as

$$D_T\psi(x) > 0 \;\forall x \in \Omega \,. \tag{4.2}$$

Therefore, let us define the quantity

$$g(x) := \begin{cases} -D_T\psi(x), & \text{if } \Psi(x) < 0, \\ D_T\psi(x), & \text{if } \Psi(x) > 0, \end{cases} \tag{4.3}$$

allowing for rewrite the condition (4.2) in the following equivalent form

$$\begin{cases} g(x) < 0, & \text{if } \Psi(x) < 0, \\ g(x) > 0, & \text{if } \Psi(x) > 0. \end{cases} \tag{4.4}$$

We observe that (4.4) is satisfied wether the quantity g coincides with the level-set function Ψ up to a strictly positive number, namely $\exists\, \tau > 0 : g = \tau\Psi$, or equivalently

$$\phi := \arccos\left[\frac{\langle g, \Psi\rangle_{L^2(\Omega)}}{\|g\|_{L^2(\Omega)}\|\Psi\|_{L^2(\Omega)}}\right] = 0 \,, \tag{4.5}$$

which shall be used as optimality condition in the topology design algorithm, where ϕ is the angle between the functions g and Ψ in $L^2(\Omega)$. Let us now explain the algorithm. We start by choosing an initial level-set function $\Psi_0 \in L^2(\Omega)$. In a generic iteration n, we compute function g_n associated with the level-set function $\Psi_n \in L^2(\Omega)$. Thus, the new level-set function Ψ_{n+1} is updated according to the following linear combination between the functions g_n and Ψ_n

$$\begin{aligned} &\Psi_0 \in L^2(\Omega), \\ &\Psi_{n+1} = \frac{1}{\sin\phi_n}\left[\sin((1-\kappa)\phi_n)\Psi_n + \sin(\kappa\phi_n)\frac{g_n}{\|g_n\|_{L^2(\Omega)}}\right] \quad \forall n \in \mathbb{N} \,, \end{aligned} \tag{4.6}$$

where ϕ_n is the angle between g_n and Ψ_n, and κ is a step size determined by a linear-search performed in order to decrease the value of the objective function $\mathcal{G}(u_n)$, with u_n used to denote the solution associated to the n-th iteration. The process ends when the condition $\phi_n \leq \epsilon$ is satisfied in some iteration, where ϵ is a given small numerical tolerance. In particular, we can choose

$$\Psi_0 \in \mathcal{S} = \{x \in L^2(\Omega); \|x\|_{L^2(\Omega)} = 1\} \,, \tag{4.7}$$

and by construction $\Psi_{n+1} \in \mathcal{S}$, $\forall n \in \mathbb{N}$. If at some iteration n the linear-search step size κ is found to be smaller then a given numerical tolerance $\epsilon > 0$ and the optimality condition is not satisfied, namely $\phi_n > \epsilon$, then a uniform mesh refinement of the hold all domain Ω is carried out and the iterative process is continued.

In this section three numerical examples of conceptual topology design of thermo-mechanical devices are presented. We assume that these devices are made of two metallic materials with similar mechanical constitutive properties and different thermal expansion coefficients. In all examples we consider the following constitutive properties: $E = 210 \times 10^3$, $\nu = 0.3$, $\alpha = 1.08 \times 10^{-5}$ and $k = 80.0$. The contrast parameter is given by $\gamma = 4.63 \times 10^{-1}$. Furthermore, the thick lines in the figures are used to denote clamped boundary conditions. In the remainder part of the boundary, where noting is specified, we consider homogeneous Neumann boundary condition. The direction e is given by a unitary vector on $\Gamma^\star$. In addition, we consider a uniform heat source given by $b = 1$. The thermo-mechanical problem (2.2), the steady-state heat conduction problem (2.9) and the adjoint equation (3.15) are solved using the standard finite element method, where uniform meshes of linear triangles are used. For the initial guess we always consider a single material with higher thermal expansion coefficient. Finally, the

black/white colors represent the materials with higher/lower thermal expansion coefficients, respectively.

4.1. **Example 1.** In this example the domain Ω is characterized by a rectangle of 2.0×1.0 of width and height, respectively, clamped on the thick line. The displacement on the middle point of the right side is to be maximized in the direction e, as shown in Fig. 3(a). The optimal distribution of materials is presented in Fig. 3(b). This result was obtained using a mesh with 12.800 elements.

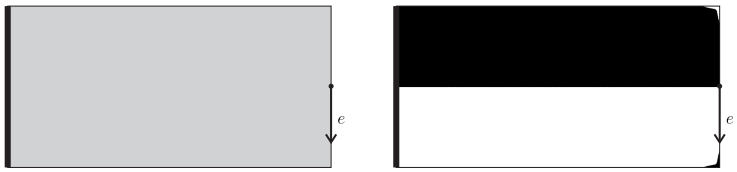

(a) (b)

FIGURE 3. Example 1: domain and boundary condition (a) and optimal material distribution (b).

In Fig. 4 is presented the evolution of the shape function $\mathcal{G}(u)$ throughout the optimization process, normalize by the Euclidian norm of the displacement of the initial guess $\|u^0\|$ evaluated on $\Gamma^\star$. Also, some intermediate topologies are shown.

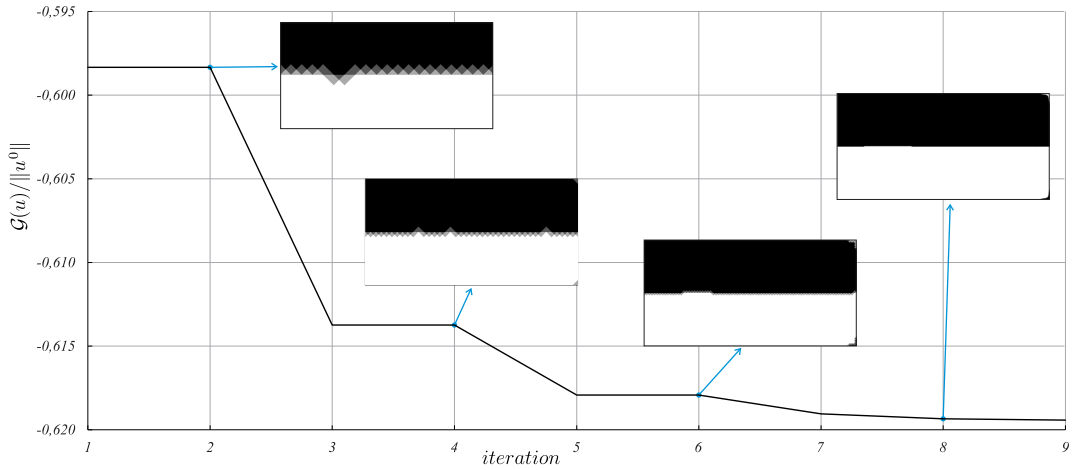

FIGURE 4. Example 1: normalized shape function vs. iterations.

The previous results indicate that the optimal material distribution is close to 50% of each one of them. Finally, the amplified deformed configurations before and after the optimization process are sketched in the Figs. 5(a) and 5(b), respectively.

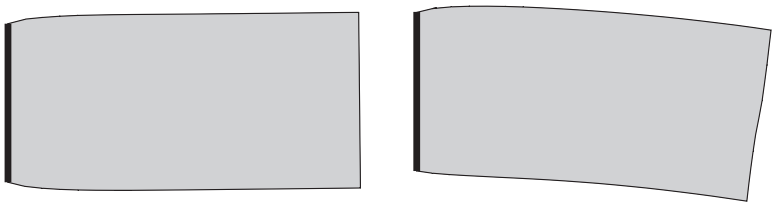

(a) (b)

FIGURE 5. Example 1: initial displacement (a) and final displacement (b).

4.2. **Example 2.** In this example we perform the optimization of a L-shaped beam, with 1.50 of height, 1.50 of length and 0.50 of width, clamped on the thick line. The direction e is defined at the corner of the L-shaped beam, as shown in Fig. 6. In this case, the angle ρ is taken between 0° and 360°. The problem is discretized into 184.320 finite elements.

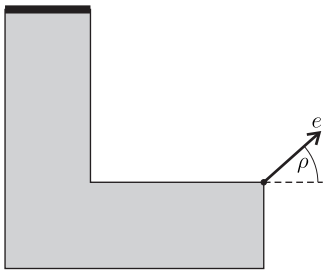

FIGURE 6. Example 2: domain and boundary condition.

In Fig. 7 are presented the following obtained results in terms of the angle ρ: the horizontal displacement u_x^{opt} (Fig. 7(a)), the vertical displacement u_y^{opt} (Fig. 7(b)), the Euclidian norm of the displacement $\|u^{opt}\|$ (Fig. 7(c)) and, finally, the volume fraction of material with higher thermal expansion material (Fig. 7(d)). Notice that in Figures 7(a) to 7(c), the results are normalized by the Euclidian norm of the displacement of the initial guess $\|u^0\|$ and all quantities are evaluated on $\Gamma^\star$. The optimal material distributions (topologies) for eight selected angles ρ are presented in Fig. 8. Finally, as an example of the deformation of the device before and after optimization, in Fig. 9 is sketched the amplified deformed configurations for $\rho = 90°$.

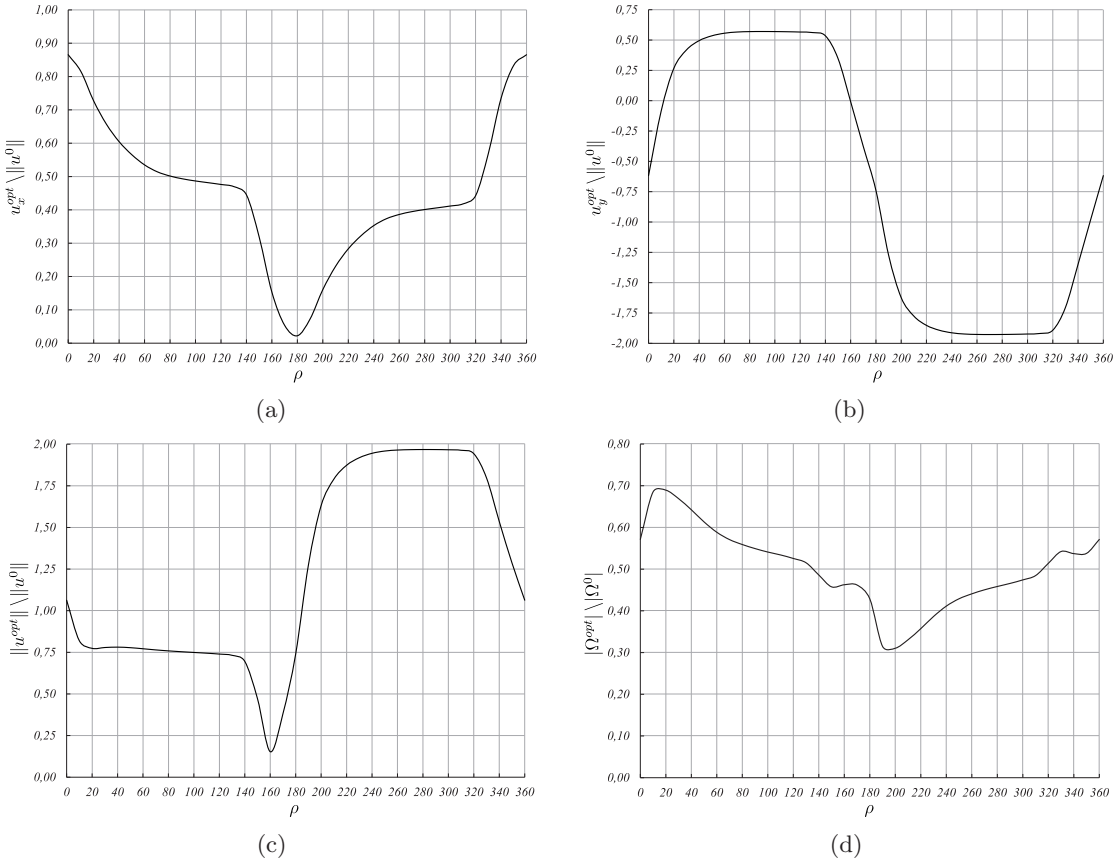

FIGURE 7. Example 2: horizontal displacement (a), vertical displacement (b), norm of the displacement (c) and final volume (d).

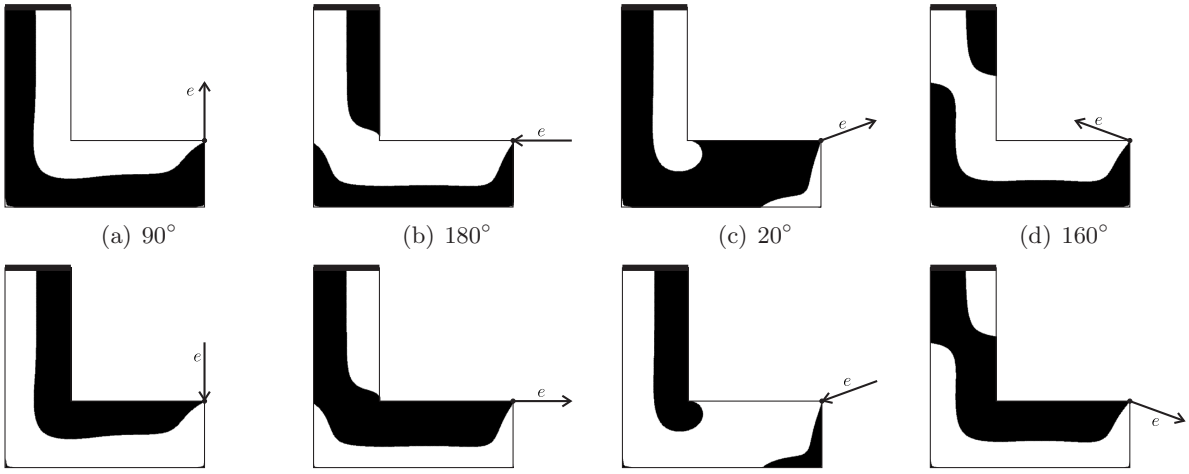

(a) 90° (b) 180° (c) 20° (d) 160°

(e) 270° (f) 0° (g) 200° (h) 340°

FIGURE 8. Example 2: obtained topologies for different angles ρ.

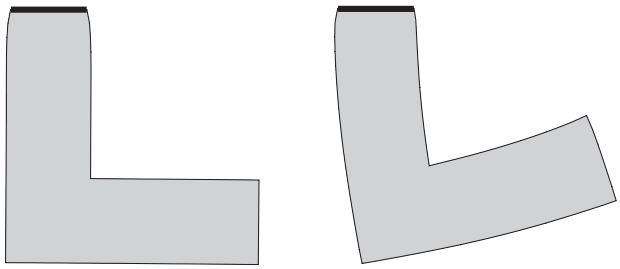

(a) (b)

FIGURE 9. Example 2: initial displacement (a) and final displacement for $\rho = 90°$ (b).

4.3. **Example 3.** In this last example we perform the optimization of a U-shaped beam, with 1.5 of height, 2.0 of length and 0.5 of width, which is simply supported in order to eliminate the rigid body motions. The displacement is to be maximized in the directions e defined at the opposite corners of the domain, as shown in Fig. 10(a). The optimal distribution of materials is presented in Fig. 10(b), where the problem has been discretized with 294.912 finite elements.

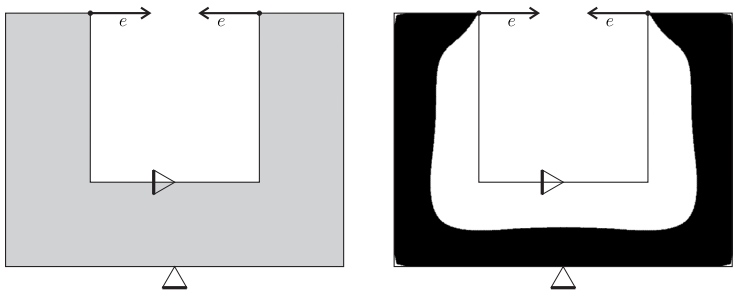

(a) (b)

FIGURE 10. Example 3: domain and boundary condition (a) and optimal material distribution (b).

In order to evaluate the influence of the finite element mesh in the optimization procedure, in Fig. 11 we present the obtained topologies for three different meshes. As can be seen through

an inspection of the figures, the meshes do not have too much influence on the results, at least from a qualitative point of view.

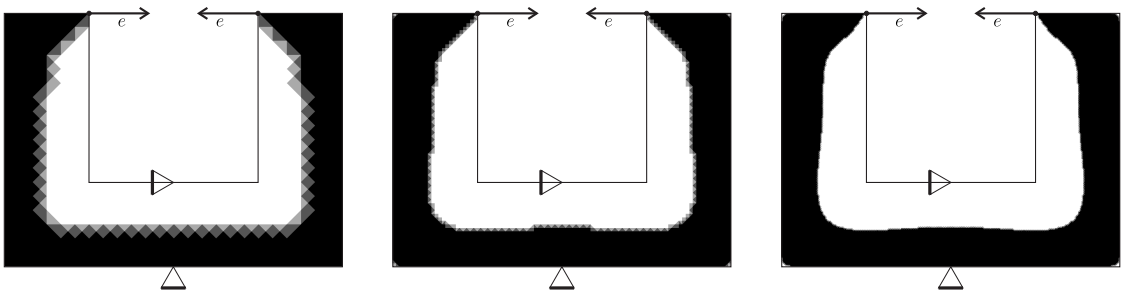

(a) 1.152 elements (b) 9.216 elements (c) 73.728 elements

FIGURE 11. Example 3: obtained topologies for different number of finite elements.

The amplified displacement of the device before and after the optimization process is sketched in the Figs. 12(a) and 12(b), respectively.

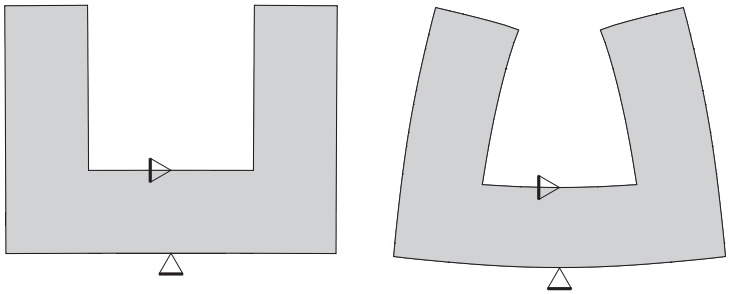

(a) (b)

FIGURE 12. Example 3: initial displacement (a) and final displacement (b).

Observe that the obtained results can be used in the conceptual design of actuators or inverters. In fact, initially the deformed configuration of the U-shaped beam is given by a simple uniform expansion. Then, after the optimization process, the new distribution of material produces a deformation similar to a grip mechanism (inverting the direction of the displacement in the top part of the beam).

5. Concluding remarks

In this work the conceptual topology design of thermo-mechanical devices has been addressed. The idea was to maximize the displacement in a given direction defined on the boundary of the thermo-elastic body with respect to a bi-metallic material distribution by introducing a set of small inclusions with different thermal expansion coefficients only. In order to avoid complicated theoretical derivations such as the ones developed in [5], the elastic properties have been fixed. By introducing a contrast only on the thermal expansion coefficients, the derivations become much simpler, allowing us to focus on the main contribution of the paper, namely, the conceptual design of bi-metallic devices using the topological derivative concept. In addition, such an incomplete sensitivity has been able to properly minimize the shape function, leading to satisfactory solutions. In other words, for the approach presented in this work, a closed form for the topological derivative associated with the nucleation of a small circular inclusion with different thermal expansion coefficient has been derived. The obtained result has been used as a steepest descent direction in an optimal design algorithm. Several numerical experiments associated with conceptual topology design of bi-metallic devices have been presented. Notice

that the proposed methodology is very simply (easy and fast numerical implementation) and does not require any additional constraint in the formulation of the optimization problem. In particular there exists an optimal distribution of the two metallic materials in the design domain without impose a constraint in the final volume fraction of any of the two phases.

Acknowledgments

This research was partly supported by the Argentinean Research and Development Program of the National Technological University (PID-UTN), and by CNPq (Brazilian Research Council) and FAPERJ (Research Foundation of the State of Rio de Janeiro). The support of these agencies is gratefully acknowledged.

References

[1] G. Allaire, F. Jouve, and N. Van Goethem. Damage and fracture evolution in brittle materials by shape optimization methods. *Journal of Computational Physics*, 230(12):5010–5044, 2011.

[2] S. Amstutz and H. Andrä. A new algorithm for topology optimization using a level-set method. *Journal of Computational Physics*, 216(2):573–588, 2006.

[3] S. Amstutz, S. M. Giusti, A. A. Novotny, and E. A. de Souza Neto. Topological derivative for multi-scale linear elasticity models applied to the synthesis of microstructures. *International Journal for Numerical Methods in Engineering*, 84:733–756, 2010.

[4] S. Amstutz, A. A. Novotny, and E. A. de Souza Neto. Topological derivative-based topology optimization of structures subject to Drucker-Prager stress constraints. *Computer Methods in Applied Mechanics and Engineering*, 233–236:123–136, 2012.

[5] S. M. Giusti, A. A. Novotny, J. E. Muñoz Rivera, and J. E. Esparta Rodriguez. Strain energy change to the insertion of inclusions associated to a thermo-mechanical semi-coupled system. *International Journal of Solids and Structures*, 50(9):1303–1313, 2013.

[6] M. Hintermüller and A. Laurain. Multiphase image segmentation and modulation recovery based on shape and topological sensitivity. *Journal of Mathematical Imaging and Vision*, 35:1–22, 2009.

[7] M. Hintermüller, A. Laurain, and A. A. Novotny. Second-order topological expansion for electrical impedance tomography. *Advances in Computational Mathematics*, 36(2):235–265, 2012.

[8] A. A. Novotny, R. A. Feijóo, C. Padra, and E. Taroco. Topological sensitivity analysis. *Computer Methods in Applied Mechanics and Engineering*, 192(7–8):803–829, 2003.

[9] A. A. Novotny and J. Sokołowski. *Topological derivatives in shape optimization*. Interaction of Mechanics and Mathematics. Springer, 2013.

[10] J. Sokołowski and A. Żochowski. On the topological derivative in shape optimization. *SIAM Journal on Control and Optimization*, 37(4):1251–1272, 1999.

[11] J. Sokołowski and J. P. Zolésio. *Introduction to shape optimization - shape sensitivity analysis*. Springer-Verlag, Berlin, Germany, 1992.

[12] N. Van Goethem and A. A. Novotny. Crack nucleation sensitivity analysis. *Mathematical Methods in the Applied Sciences*, 33(16):197–1994, 2010.

(S.M. Giusti) Universidad Tecnológica Nacional, Facultad Regional Córdoba UNT/FRC - CONICET, Maestro M. López esq. Cruz Roja Argentina, X5016ZAA - Córdoba, Argentina.
E-mail address: sgiusti@civil.frc.utn.edu.ar

(A.A. Novotny) Laboratório Nacional de Computação Científica LNCC/MCTI, Coordenação de Matemática Aplicada e Computacional, Av. Getúlio Vargas 333, 25651-075 Petrópolis - RJ, Brasil.
E-mail address: novotny@lncc.br